Deterministic microfluidic ratchet based on the deformation of individual cells

Quan Guo,[1] Sarah M. McFaul,[1] and Hongshen Ma[1,2,3,*]

[1]*Department of Mechanical Engineering, University of British Columbia, 2054-6250 Applied Science Lane, Vancouver, British Columbia, Canada V6T 1Z4*

[2]*Department of Urologic Science, University of British Columbia, Vancouver, British Columbia, Canada V5Z 1M9*

[3]*Vancouver Prostate Centre, Vancouver General Hospital, Vancouver, British Columbia, Canada V5Z 1M9*

(Received 5 February 2011; published 11 May 2011)

We present a microfluidic ratchet that exploits the deformation of individual cells through microscale funnel constrictions. The threshold pressure required to transport single cells through such constrictions is greater against the direction of taper than along the direction of taper. This physical asymmetry combined with an oscillatory excitation can enable selective and irreversible transport of individual cells in low Reynolds number flow. We devised a microfluidic device to measure the pressure asymmetry across various geometries of funnel constrictions. Using a chain of funnel constrictions, we showed that oscillatory pressure enables ratcheting transport when the pressure amplitude and oscillation period exceeds the threshold required to transport single cells. These experiments demonstrate the potential of using this mechanism to selectively transport biological cells based on their internal mechanics, and the potential to separate cells based on cell morphology or disease state.

DOI: 10.1103/PhysRevE.83.051910 PACS number(s): 87.85.Ox, 83.50.−v, 87.19.rh, 87.85.G−

Microscale ratchet mechanisms use a periodic structure with local asymmetry and local excitation to overcome kinematic reversibility associated with small-scale inertialess Stokes flows and generate rectified motion of individual particles against the viscous drag of its carrier fluid [1,2]. When the magnitude of the local asymmetry depends on physical properties of particles, such as size and deformability, ratchet mechanisms can be used to selectively transport particles based on specific physical characteristics. This capability could address a variety of cell separation and cell analysis challenges related to diseases such as malaria and cancer, where there are established relationships between disease status and the physical properties of individual cells [3–7].

Previous studies have demonstrated ratchet mechanisms that exploit asymmetries based on electrical potential [8], dielectrophoresis [9,10], optical traps [11], contact forces between microparticles and obstacles [12,13], and bacteria and cell motility [14–16]. The asymmetries found in these cases are strongly coupled with particle size, and therefore ultimately useful for size-based separation [17]. Since the sizes of biological cells are generally associated with the diffusion of nutrients from the surrounding environment, cell size is often poorly correlated with physiological properties. Thus, sorting of cells based on properties other than size remains a desirable goal. The deformability of cells, on the other hand, is related to the composition of the cytoplasm and the structure of the cytoskeleton, and as a result can vary by orders of magnitude depending on cell type and disease status [18,19]. If cell deformability could be coupled with a local asymmetry to form a microscale ratchet, such a mechanism could be used to selectively transport cells based on differences in their internal mechanics, and to separate or sort cells based on morphology or disease status.

In this paper, we present a microscale ratchet mechanism where the local asymmetry is coupled to the deformability of individual cells through microscale funnel constrictions (Fig. 1). Compressing cells through this constriction along the direction of the taper (the "forward" direction) requires a smaller applied pressure than against the taper (the "reverse" direction). Therefore, applying an unbiased square wave pressure oscillation with amplitude above the necessary forward threshold pressure enables rectified transport along the direction of the taper. A millimeter-scale version of this mechanism used to deform mercury droplets has been reported previously [20]. This paper studies the properties of various funnel structures at the length scale of biological cells and examines the potential of using structural interactions to modify the flow behavior of individual cells.

The threshold pressure required to deform a single cell through a microscale funnel constriction can be modeled by considering the cell as a liquid-filled sac with constant cortical tension [18]. The end-to-end pressure required to quasistatically form the leading and trailing surfaces in the constriction is determined by an application of the Young-Laplace law and gives

$$\Delta P = 2T_C \left(\frac{1}{R_a} - \frac{1}{R_b} \right), \tag{1}$$

where ΔP is the pressure difference, T_C is the cortical tension of the membrane (assumed to be isotropic and constant), and R_a and R_b are the radii of the leading and the trailing surfaces, respectively. As the leading edge of the cell is pulled into the constriction, ΔP eventually reaches a maximum and then decreases upon further deformation. This phenomenon causes an instability known as a Haines jump, whereby the entire cell is pulled rapidly into the microstructure [21]. Since $R_b \gg R_a$, the Haines jump instability occurs near $R_a = W_0/2$, whereas the corresponding value of R_b can be determined from volume conservation. The required pressure asymmetry between deforming cells in the forward and reverse directions arises from the geometrical constraints imposed by the microstructure. Specifically, when cells are deformed in the forward direction, the presence of the funnel sidewalls reduces

*Author to whom correspondence should be addressed: hongma@mech.ubc.ca

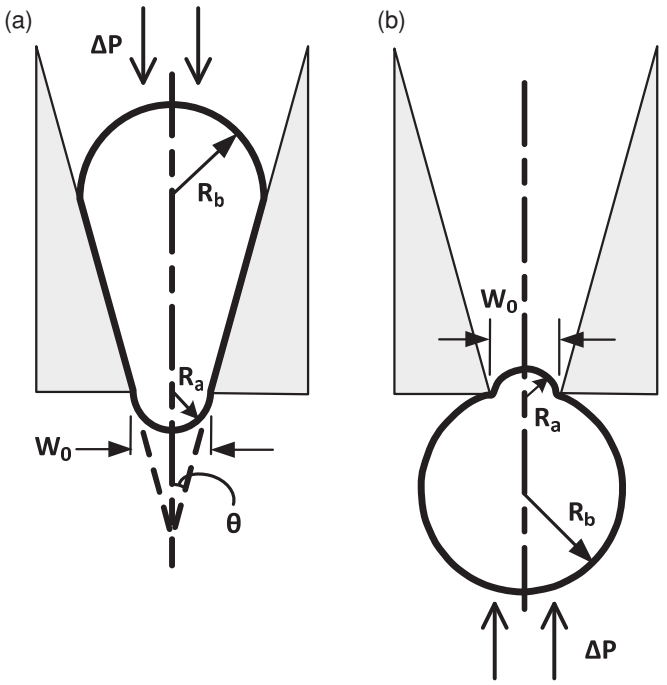

FIG. 1. Deformation of a single cell through microscale funnel constrictions in forward and reverse directions. Key parameters of the microstructure include the funnel pore size (W_0) and half-angle of the funnel taper (θ).

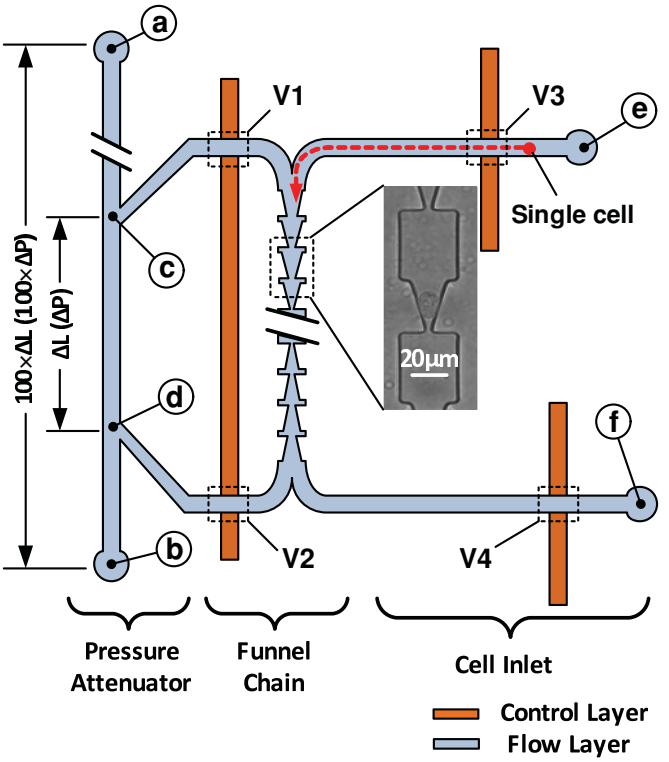

FIG. 2. (Color online) Design of a two-layer microfluidic device for measuring the pressure required to deform single cells through microscale funnel constrictions. An upper flow layer comprises two sets of 10 funnels arranged in opposite polarity and decreasing in pore size toward the center of the chain. Single cells are introduced at (e) and (f), and then deformed through the funnel chain using the pressure difference between (c) and (d), which is attenuated 100 times from the external pressure applied across (a) and (b). The pressure application and cell inlet processes are activated using the control layer valves V1–V4.

the value of R_b and therefore requires a smaller ΔP value to reach the condition for a Haines jump as compared to when cells are deformed in the reverse direction.

To measure the pressure difference required to deform single cells both ways through various-sized funnel constrictions, we developed a microfluidic device using multilayer soft lithography of polydimethylsiloxane [22,23]. Shown in Fig. 2, this device contains a central microchannel where funnels with $W_0 = 11, 10, 9, 8, 7, 6, 5, 4, 3.5$, and $3\ \mu$m are arranged in series from the distal end of the microchannel to its center, and then mirrored from the center of the microchannel to the opposing distal end. Using many funnels in one microchannel enables experiments with varying funnel geometries to be conducted on the same cell. Mirroring the funnel chain design at the center of the microchannel eliminates any possible asymmetrical hydrodynamic resistance to the bulk fluid [24]. This design is replicated for funnels tapered at 10°, 5°, and 0°. The height of the microchannels is approximately 16 μm, which exceeds the typical diameter of cells used in our experiments.

The chain of funnel is connected to parallel microchannel networks for introducing individual cells from a sample reservoir and for applying an attenuated pressure across the funnel chain. These two networks are isolated from each other using microvalves V1–V4 so that the introduction of cells and the pressure deformation process can take place independently. Pressure attenuation is accomplished using a fluidic circuit similar to a resistive divider used in electronic circuits. As shown in Fig. 2, pressure from an external source is applied across points (a) and (b) on a long microchannel. Side branches located at points (c) and (d) are spaced at 1/100 of the distance from (a) to (b), and therefore attenuate the applied pressure by a factor of 100. Microchannel networks connected to the side branch do not significantly affect the pressure drop across (c) and (d) as long as the hydrodynamic resistance of the network is significantly greater than that of the microchannel segment between (c) and (d).

The pressures required to deform single cells through various funnel microstructures were measured using the following process: A single cell is introduced into the main microchannel with valves V1 and V2 sealed and valves V3 and V4 open. Once the cell flows into the funnel region, the states of all four valves are inverted, exposing the funnel array to the attenuated pressure applied across (c) and (d). This pressure is raised gradually in increments of 5 Pa until the cell successfully transits through successive constrictions. The experimental process is shown in [25]. After traversing through a given funnel constriction, the cell is then given ~30 s to recover its original shape before a subsequent measurement.

L1210 mouse lymphoma cells (MLCs), with cell diameters (Φ_{cell}) ranging from 8 to 12 μm, are used to study the performance of the funnel ratchet. The forward and reverse threshold pressures required to squeeze single cells through funnel constrictions tapered at 10° plotted as a function of W_0 are shown in Fig. 3(a). The asymmetry between the forward and reverse threshold pressure required for ratcheting is clearly observed. The measured threshold pressures were remarkably

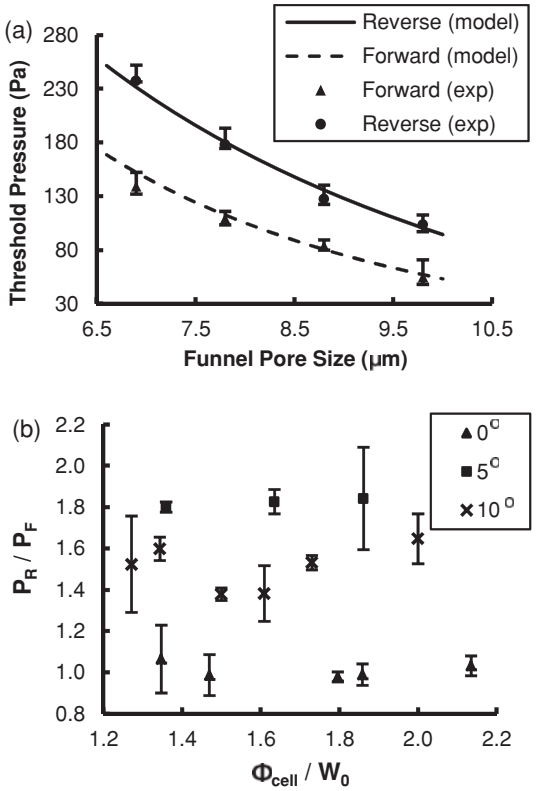

FIG. 3. (a) Forward and reverse threshold pressures required to deform a single MLC ($\Phi_{cell} = 15.6\ \mu$m) through a 10° funnel constriction. The model curves have been fitted using a cortical tension of 750 pN/μm. (b) Pressure asymmetry for 10°, 5°, and 0° funnel constrictions as a function of Φ_{cell}/W_0. Data points shown are the average pressures from 3–4 measurements on the same cell, while the error bar shows the range of the measured results.

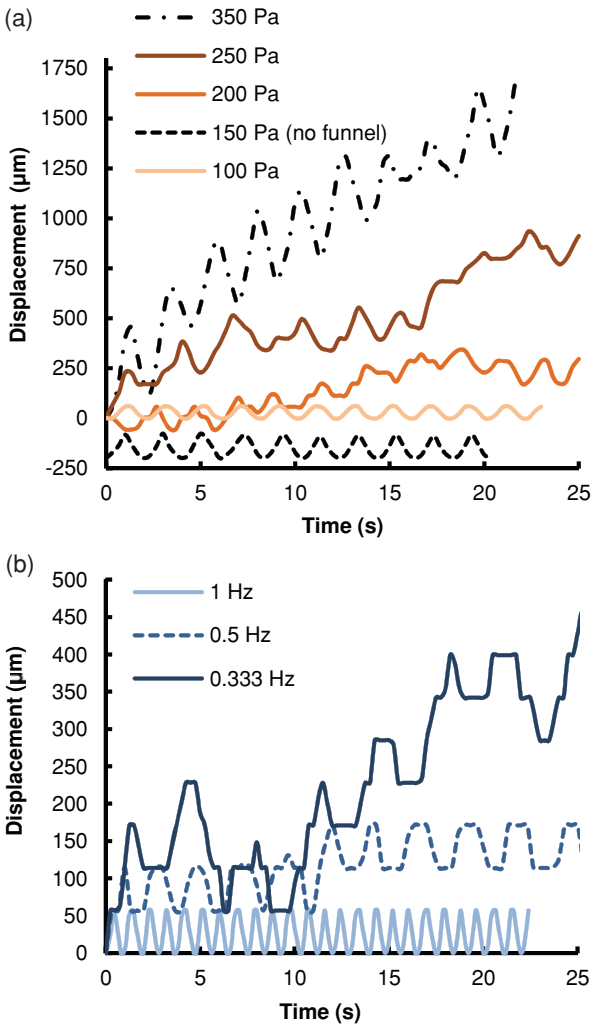

FIG. 4. (Color online) (a) The displacement of a single MLC ($\Phi_{cell} = 10.5\ \mu$m) in the funnel chain ($W_0 = 6\ \mu$m) with a 0.5 Hz oscillation at various pressure amplitudes. An offset has been added to the initial positions of these curves such that they begin at the same point. The no-funnel curve is a control experiment that tracks the cell motion in an unconstrained microchannel prior to entering the funnel chain. (b) Frequency dependence of ratchet motion with an oscillation pressure amplitude of 150 Pa.

repeatable for the same cell, which suggests that this device could be used to study single cell biomechanics in a fashion similar to micropipette aspiration [18]. The liquid-drop model given by Eq. (1), modified for the constraint provided by the funnel constriction using a similar approach as for tapered micropipettes [26], has been fitted to the experimental data by adjusting the value of T_C. The resulting value for the cortical tension of MLCs is 750 pN/μm, which is comparable to values obtained for mammalian eukaryotic cells in previous studies using micropipette aspiration [27]. The pressure asymmetry results measured from the deformation of MLCs are shown in Fig. 3(b) as a nondimensional plot of the reverse-to-forward pressure ratio (P_R/P_F) versus the cell-diameter-to-funnel-opening ratio (Φ_{cell}/W_0) for funnel constrictions tapered at 10°, 5°, and 0°. As expected, smaller funnel angles yield greater asymmetry because of the more gradual taper. The average asymmetry values for the 5° funnel and the 10° funnel are approximately 1.8 and 1.5, respectively. The 0° funnel is simply a 20 μm long rectangular slot constriction. Deforming cells through these control constrictions showed no pressure asymmetry ($P_R/P_F \approx 1.0$), which confirms the lack of inherent asymmetries in the measurement apparatus.

To study the ratchet transport of single cells in microscale funnel constrictions, we designed and fabricated a modified version of the microfluidic device consisting of 37 funnels of identical geometries arranged in series at a pitch of 60 μm. The chain of funnel microstructures is connected to the pressure attenuator and the cell inlet as before. The pressure attenuator contains four additional microvalves that act as a fluidic H-bridge to enable rapid reversal of the source pressure polarity. Integrating this feature on-chip eliminates the time delay associated with inverting the applied pressure using an external source. Single cells are introduced into this funnel chain through the inlet network. Once a cell reaches the funnel chain, an unbiased oscillatory pressure is applied. The motion of an individual MLC through the chain of funnel constrictions is tracked by video analysis. The microscope stage is moved manually to follow the motion of the cell while using fiducial markings on the side of the funnel chain to track the global position of the cell in the funnel chain.

The displacements of single MLCs in a funnel chain for several different amplitudes of the square-wave oscillatory

pressure are shown in Fig. 4(a) and the process is documented in the video in [28]. The funnel pore size in this device is 6 μm, while the pressure oscillation frequency is 0.5 Hz. This graph also includes cell displacement data from a control experiment where the oscillatory pressure was applied to a MLC in a section of the central microchannel prior to entering the funnel chain. The unbiased sinusoidal cell displacement shown here confirms the unbiased oscillatory fluid flow of the bulk fluid.

Ratcheting behavior is observed when the pressure amplitude exceeds the threshold required to deform MLCs across a single funnel constriction along the direction of the taper. Specifically, at amplitude of 100 Pa, cells are confined to oscillate in the region between two funnels, but at 200 Pa and above the cell begins to ratchet forward in the funnel chain in a reliable and deterministic fashion, as shown in Fig. 4(a). The observed threshold for ratcheting is consistent with the forward and reverse pressure thresholds shown in Fig. 3(a), which are 165 and 220 Pa, respectively, for $\Phi_{\text{cell}} = 10.5$ μm and $W_0 = 6$ μm. Above 200 Pa, the cell travels both forward and backward through several funnel constrictions in each cycle. Ratcheting behavior is preserved at these higher oscillation pressure amplitudes since the asymmetrical threshold pressure enables these cells to transit through a great number of funnels in the forward direction rather than the backward direction. The increased applied pressure also increases the net cell velocity. The average flow velocity for pressure amplitudes of 200, 250, and 350 Pa is 15, 30, and 60 μm/s, respectively.

The ratcheting behavior is found to depend on oscillation frequency as shown in Fig. 4(b). At a frequency of 1 Hz and an amplitude of 150 Pa, the cells do not have sufficient time to traverse the region between the funnels ($\sim$50 μm) and also deform across the funnel. Ratcheting transport is enabled at 0.5 Hz, and proceeds at an increased net forward velocity at 0.333 Hz, suggesting that $\sim$0.5 s is required to complete the process to deform through the funnel constriction. The ratcheting process is also dependent on the synchronization between the applied pressure and the location of the cell in a funnel constriction, as well as surface forces between the cell and the microstructure.

In summary, we investigated the properties of a microfluidic ratchet based on the deformation of single cells through microscale funnel constrictions. Threshold pressures required to squeeze single cells through such microstructures showed strong directional asymmetry. Rectified motion of cells was observed in a funnel chain from an unbiased oscillatory flow when the applied oscillation pressure and time period exceeded the thresholds required to squeeze single cells through individual funnel microstructures. This mechanism is deterministic and repeatable and can be modeled in simple terms. Cell deformation, not cell size, is coupled with the local asymmetry and used to produce rectified motion. Since microfluidic technologies can now provide exquisite control of the pressure and flow rate of fluids within complex microstructures, we believe this mechanism can form the basis of deformability-based cell separation devices, as well as devices for measuring the stiffness of individual cells.

The authors acknowledge L. C. So and I. Tang for fabrication assistance, E. Polishchuk for providing the L1210 cell line, and G. M. Homsy for valuable discussions. This work was supported by grants from the National Science and Engineering Research Council of Canada, the Bill and Melinda Gates Foundation Grand Challenges in Global Health program, Genome British Columbia, and the PC-TRIADD Centre of Excellence in Research and Commercialization at the Vancouver Prostate Centre. S.M. acknowledges support from the Michael Smith Foundation for Health Research.

[1] R. D. Astumian, Science **276**, 917 (1997).
[2] F. Julicher, A. Ajdari, and J. Prost, Rev. Mod. Phys. **69**, 1269 (1997).
[3] H. A. Cranston, C. W. Boylan, G. L. Carroll, S. P. Sutera, J. R. Williamson, I. Y. Gluzman, and D. J. Krogstad, Science **223**, 400 (1984).
[4] S. E. Cross, Y. S. Jin, J. Tondre, R. Wong, J. Rao, and J. K. Gimzewski, Nanotechnology **19**, 384003 (2008).
[5] G. B. Nash, E. Obrien, E. C. Gordonsmith, and J. A. Dormandy, Blood **74**, 855 (1989).
[6] S. Suresh, J. Spatz, J. P. Mills, A. Micoulet, M. Dao, C. T. Lim, M. Beil, and T. Seufferlein, Acta Biomater. **1**, 15 (2005).
[7] W. A. Lam, M. J. Rosenbluth, and D. A. Fletcher, Blood **109**, 3505 (2007).
[8] J. S. Bader, R. W. Hammond, S. A. Henck, M. W. Deem, G. A. McDermott, J. M. Bustillo, J. W. Simpson, G. T. Mulhern, and J. M. Rothberg, Proc. Natl. Acad. Sci. USA **96**, 13165 (1999).
[9] L. Gorre-Talini, J. P. Spatz, and P. Silberzan, Chaos **8**, 650 (1998).
[10] J. Rousselet, L. Salome, A. Ajdari, and J. Prost, Nature (London) **370**, 446 (1994).
[11] L. P. Faucheux, L. S. Bourdieu, P. D. Kaplan, and A. J. Libchaber, Phys. Rev. Lett. **74**, 1504 (1995).
[12] K. Loutherback, J. Puchalla, R. H. Austin, and J. C. Sturm, Phys. Rev. Lett. **102**, 045301 (2009).
[13] S. Matthias and F. Muller, Nature (London) **424**, 53 (2003).
[14] P. Galajda, J. Keymer, J. Dalland, S. Park, S. Kou, and R. Austin, J. Mod. Opt. **55**, 3413 (2008).
[15] S. E. Hulme, W. R. DiLuzio, S. S. Shevkoplyas, L. Turner, M. Mayer, H. C. Berg, and G. M. Whitesides, Lab Chip **8**, 1888 (2008).
[16] G. Mahmud, C. J. Campbell, K. J. M. Bishop, Y. A. Komarova, O. Chaga, S. Soh, S. Huda, K. Kandere-Grzybowska, and B. A. Grzybowski, Nat. Phys. **5**, 606 (2009).
[17] J. A. Davis, D. W. Inglis, K. J. Morton, D. A. Lawrence, L. R. Huang, S. Y. Chou, J. C. Sturm, and R. H. Austin, Proc. Natl. Acad. Sci. USA **103**, 14779 (2006).
[18] R. M. Hochmuth, J. Biomech. **33**, 15 (2000).
[19] C. T. Lim, E. H. Zhou, and S. T. Quek, J. Biomech. **39**, 195 (2006).
[20] L. Gorre, E. Ioannidis, and P. Silberzan, Europhys. Lett. **33**, 267 (1996).
[21] W. B. Haines, J. Agric. Sci. **20**, 97 (1930).

[22] M. A. Unger, H. P. Chou, T. Thorsen, A. Scherer, and S. R. Quake, Science **288**, 113 (2000).
[23] V. Studer, G. Hang, A. Pandolfi, M. Ortiz, W. F. Anderson, and S. R. Quake, J. Appl. Phys. **95**, 393 (2004).
[24] A. Groisman and S. R. Quake, Phys. Rev. Lett. **92**, 094501 (2004).
[25] See supplemental material at [http://link.aps.org/supplemental/10.1103/PhysRevE.83.051910] for movie S1: Pressure asymmetry measurement.
[26] D. Needham and R. M. Hochmuth, Biophys. J. **61**, 1664 (1992).
[27] J. Y. Tinevez, U. Schulze, G. Salbreux, J. Roensch, J. F. Joanny, and E. Paluch, Proc. Natl. Acad. Sci. USA **106**, 18581 (2009).
[28] See supplemental material at [http://link.aps.org/supplemental/10.1103/PhysRevE.83.051910] for movie S2: Rectified cell motion in the funnel chain.